Lumped-Element Circuit Modelling of Microfluidic Channels in Microstrip Transmission Lines

Matthew Brown, Ian Goode, Carlos E. Saavedra
Department of Electrical and Computer Engineering
Queen's University, Kingston, Ontario, Canada K7L 3N6

***Abstract*—A lumped-element equivalent circuit model (ECM) for a short length of microstrip transmission line incorporating a microfluidic channel filled with dielectric fluid is proposed. With this model, advanced microstrip circuits containing microfluidic channels can be designed in a fast and accurate manner. For verification, an ECM is extracted for a 1-mm length of 50 Ω transmission line on a 1.5-mm thick substrate with $\epsilon_r = 3.55$ that has a 0.5-mm long $\times$ 0.5-mm tall $\times$ 6.9-mm wide microfluidic channel underneath it filled with a dielectric fluid of $\epsilon_r = 81$. The model parameter values are extracted using the structure's two-port S-parameter response obtained through full-wave 3D electromagnetic simulation. The extracted ECM is then used to design a fluidic phase shifter.**

***Index Terms*—dielectric fluid, electromagnetic simulation, equivalent circuit model, fluidics, lumped-element, microfluidics, microstrip, microwaves, phase shifter, time-delay**

I. Introduction

In recent years the use of dielectric fluids flowing in microchannels (microfluidics) to tune microwave circuits and antennas systems has increased [1]. The introduction of fluid changes the local relative permittivity of the microstrip, which changes the response of the structure. The ability to add and remove different fluids with significantly different dielectric constants opens the possibility for multiple responses to be achieved with the same circuit. The use of microfluidic tuning has been used for variable phase shifters[2], [3], filters[4], [5], antennas [6], [7] and frequency selective surfaces [8].

The design of microwave microfluidic circuits currently relies on time-intensive 3D full-wave electromagnetic (EM) simulations. In view of the wide variety of microwave microfluidic circuits that are being investigated and reported in the literature, a compact ECM for a microfluidic *unit element* for schematic-level simulation can save significant amounts of time leading up to full-wave simulation and fabrication.

This paper presents a π-network ECM for a short length of microstrip tranmission line and microfluidic channel filled with dielectric fluid. To the author's knowledge, this is the first circuit model to be proposed for a microwave microfluidic subcomponent. The model is verified by extracting an ECM of a microfluidic microstrip unit element and using the ECM to design a tunable phase shifter at the schematic level using the Keysight ADS simulator. The phase shifter results are then compared against full-wave EM simulations using ANSYS HFSS.

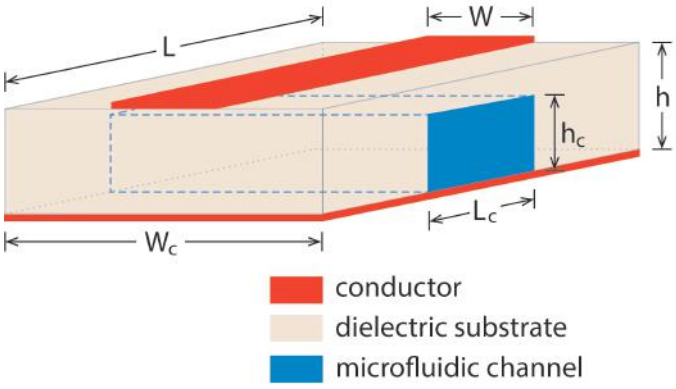

Fig. 1: Diagram of a short length of microstrip transmission line loaded with a fluidic channel underneath.

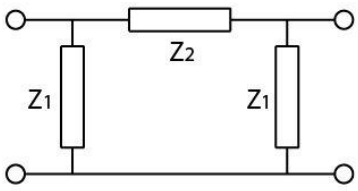

(a)

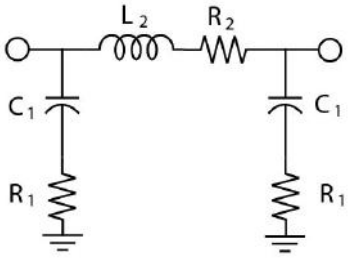

(b)

Fig. 2: (a) Proposed lumped-element π-model for a short length of transmission line and fluidic channel and (b) The full equivalent circuit model (ECM) including losses.

II. Equivalent Circuit Model

The short length of transmission line with microfluidic channel that is chosen for modelling is depicted in Fig. 1. The channel width, W_c, spans the entire width of the microstrip substrate and is located directly above the ground plane. A layer of substrate separates the transmission line metal from

TABLE I: Transmission Line and Channel Dimensions

Variable	W	L	h	W_c	L_c	h_c
(mm)	3.45	1.00	1.52	6.90	0.50	0.50

TABLE II: Parameters Calculated for ECM

Variable	$C_1(fF)$	$L_2(pH)$	$R_1(\Omega)$	$R_2(m\Omega)$
Value	124.33	418.32	1.85	47.50

the channel of thickness $h - h_c$, where h is the height of the substrate and h_c is the height of the fluidic channel. The proposed ECM for the transmission line and channel is a lumped-element π network as shown in Fig. 2a. It is a symmetric network where the shunt elements are equal to each other. The model can be used with a wide range of transmission line/microfluidic geometries (e.g. round channels, vertical channels etc). Fig. 2b shows the detailed circuit model.

The $ABCD$ matrix of the lumped network is

$$\begin{bmatrix} A & B \\ C & D \end{bmatrix} = \begin{bmatrix} 1 + Z_2Y_1 & Z_2 \\ 2Y_1 + Y_1^2Z_2 & Y_1Z_2 + 1 \end{bmatrix}. \quad (1)$$

From this matrix, the lumped-element values are calculated as

$$Z_1 = B/(A-1) \quad \text{and} \quad Z_2 = B \quad (2)$$

and reformulating these two expressions in terms of scattering parameters yields

$$Z_1 = \frac{(1+S_{11})(1+S_{22}) - S_{12}S_{21}}{(1+S_{11})(1-S_{22}) + S_{12}S_{21} - 2S_{21}} = R_1 + jX_1 \quad (3)$$

$$Z_2 = \frac{(1+S_{11})(1+S_{22}) - S_{12}S_{21}}{2S_{21}} = R_2 + jX_2 \quad (4)$$

Once the S-parameters of the physical structure in Fig. 1 have been found through measurement or full-wave simulation, Z_1 and Z_2 are calculated using Eqs. (3)-(4).

III. Verification

A. Model extraction

An ECM for the structure in Fig. 1 is extracted for the case of a 50 Ω transmission line on a 1.52-mm thick substrate with $\epsilon_r = 3.55$ and a loss tangent of 0.0027 (Rogers Corp. 4003C). The fluidic channel underneath is filled with distilled water, $\epsilon_r = 81$ at room temperature. The physical dimensions of the structure are shown in Table I.

The structure was simulated using ANSYS HFSS over the range of 4 to 6 GHz at the center frequency of 5 GHz ($\lambda_g = 36$ mm). The mesh setup had a lambda refinement of 0.2 with a maximum refinement per pass of 20%. From the dimensions in Table I, note that the ratio $L/\lambda_g = 1.0/36 = 0.028$ which is consistent with the objective of simulating a short transmission line segment. The HFSS S-parameter simulation results and subsequent calculation of the impedances using Eqs. (3) and (4) shows that, as expected, the imaginary part of Z_1 is capacitive and the imaginary part of Z_2 is inductive. Thus, the lumped-element capacitor and inductor components are found using,

$$C_1 = \frac{-1}{2\pi f X_1} \quad \text{and} \quad L_2 = \frac{X_2}{2\pi f} \quad (5)$$

The values of C_1 and L_2 over the 4 to 6 GHz band from the HFSS S-parameter data are 124.3 ± 1 fF and 418.3 ± 3 pH, respectively. The resistive components, R_1 and R_2 are found by taking an average value of the real part of Eqs. (3) and (4) and their values are $R_1 = 1.85\ \Omega$ and $R_2 = 47.5$ mΩ.

The ECM model parameters are summarized in Table II and Fig. 3 shows the difference in the S-parameters for the short-length of transmission line with the fluidic channel from the HFSS simulation and the ECM model prediction.

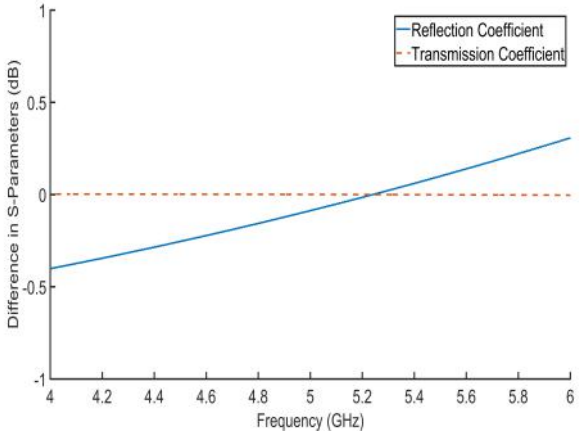

Fig. 3: Differences in the reflection and transmission coefficient between the HFSS results and ECM for the short piece of transmission line with fluidic channel.

B. Phase Shifter

As a test case to verify the predictive capability of the ECM, a fluidic microstrip phase shifter was designed on the same substrate as before. The phase shifter has three fluidic channels of length L_c separated by a distance L_2. The circuit was simulated using the Keysight ADS schematic environment using transmission lines and the lumped-element ECM derived in earlier for the fluidic channels is depicted in Fig. 4a. The phase shifter was subsequently simulated in HFSS. The top view of the HFSS model is depicted in Fig. 4b including the transmission line and channel dimensions and Fig. 4c shows the 3D rendering of the simulation space.

Fig. 5 shows the S-parameter phase response of the fluidic phase shifter from the HFSS full-wave simulation and from the ECM prediction from ADS.

Meanwhile, Figs. 6 and 7 show the magnitudes of the transmission and reflection coefficients for both the HFSS and ADS results, respectively.

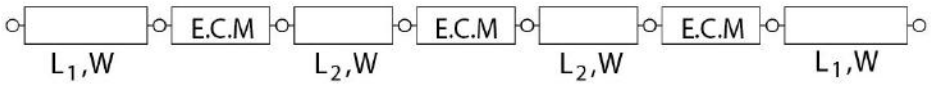

(a)

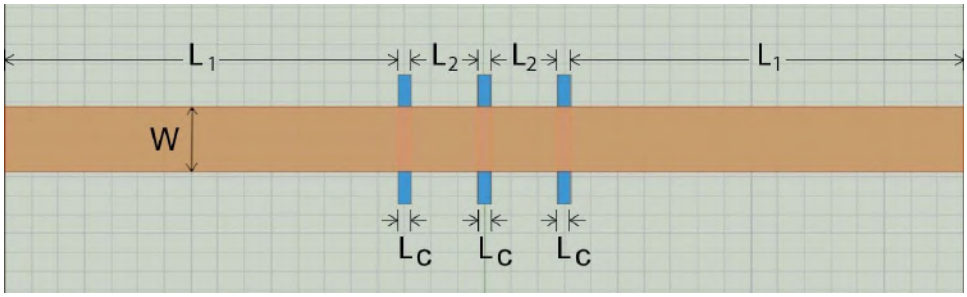

dimension	W	L_c	L_1	L_2
(mm)	3.45	1.0	14.5	2.0

(b)

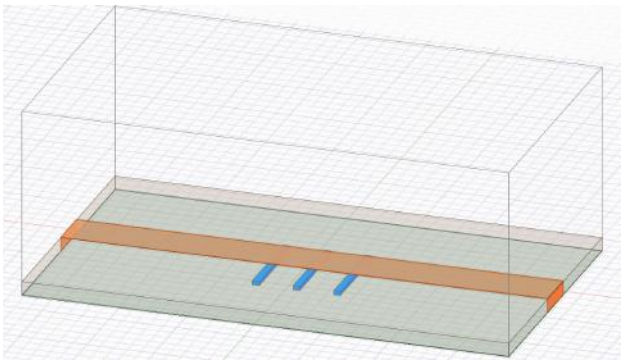

(c)

Fig. 4: (a) ADS schematic model, where the derived ECM is connected with transmission lines (b) HFSS model top view of fluidic phase shifter with three channels and (c) HFSS simulation boundary.

Fig. 8 and 9 shows the difference in the phase and magnitude of the transmission and reflection coefficients for both models respectively.

The maximum difference between the two models over the entire 4-6 GHz band for the phase of the reflection and transmission coefficient is $4.9°$ and $1.4°$ respectively. The maximum difference for the magnitude of the reflection and transmission coefficients over the entire band is 5.90 dB and 0.49 dB respectively.

The average difference in phase over the 4-6 GHz band between the two models for the reflection and transmission coefficients is $2.97°$ and $0.22°$ respectively. While the average difference in magnitude between the two models for the reflection and transmission coefficients is 3.7 dB and 0.44 dB respectively. The results are summarized in Table III.

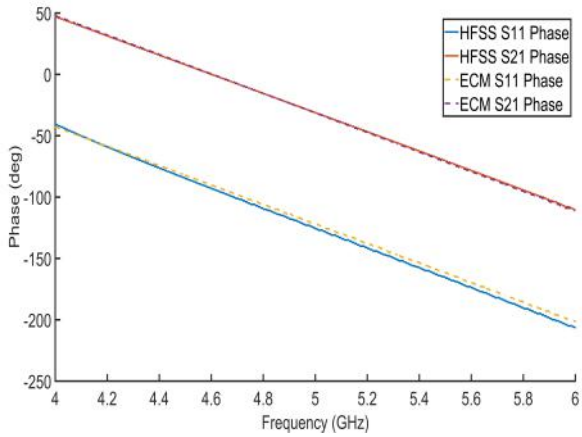

Fig. 5: Phase response for the phase shifter for both the HFSS results and ECM.

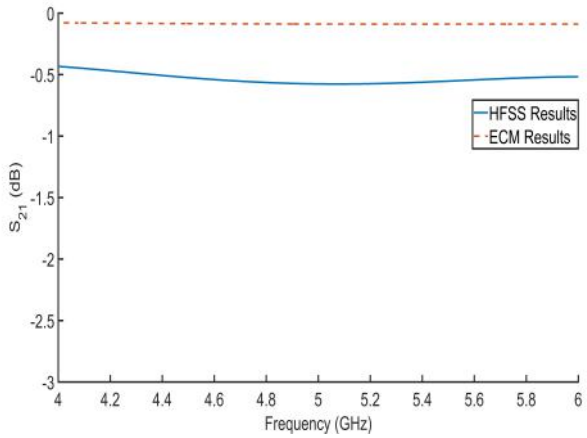

Fig. 6: Transmission coefficient for the HFSS results and ECM for the phase shifter with three fluidic channels.

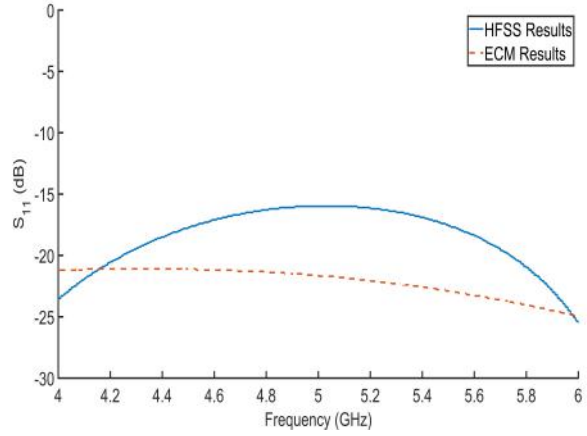

Fig. 7: Reflection coefficient for the HFSS results and ECM for the phase shifter with three fluidic channels.

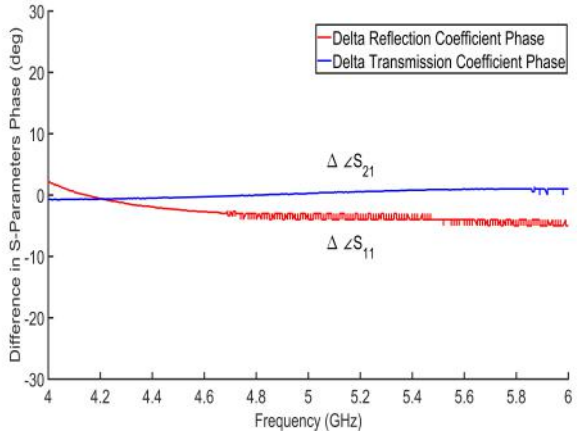

Fig. 8: Differences between the HFSS results and ECM for the phase of the reflection and transmission coefficients, for the phase shifter with three fluidic channels.

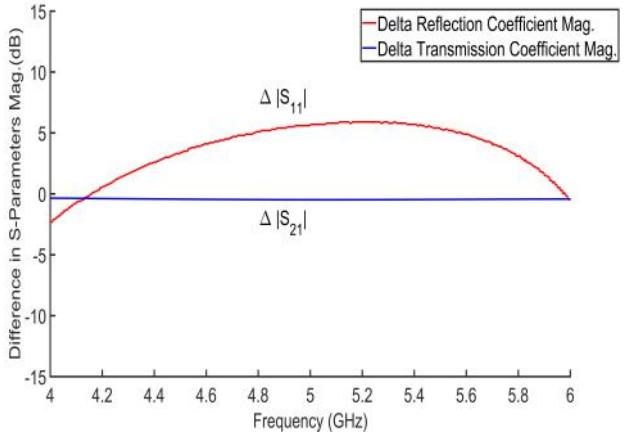

Fig. 9: Differences between the HFSS results and ECM for the magnitude of the reflection and transmission coefficients, for the phase shifter with three fluidic channels.

TABLE III: Phase shifter average variation between HFSS and ECM prediction

Variable	$\angle S_{11}(^\circ)$	$\angle S_{21}{}^\circ$	$\lvert S_{11}\rvert$ (dB)	$\lvert S_{21}\rvert$ (dB)
Difference	2.97	0.22	3.70	0.44

IV. Conclusions

The author's have shown that the proposed equivalent circuit model of a microfluidic unit element has substantial predictive capabilities as demonstrated by the subsequent design of a fluidic-phase shifter. A wide range of microwave microfluidic unit-element geometries can be modelled using the ECM proposed in this paper. Thus, a designer can generate library of ECMs for the preferred geometries and used them in a schematic simulator.

References

[1] K. Entesari and A. P. Saghati, "Fluidics in Microwave Components," *IEEE Microwave Magazine*, vol. 17, no. 6, pp. 50-75, June 2016.

[2] L. Le Cloirec, A. Benlarbi-Delai, and B. Bocquet, "3 bit 90-deg millimeter phase shifter using microfluidic technology," *Eur. Microw. Conf.* vol. 3, pp. 14, 2004.

[3] Goode. Ian, Saavedra. Carlos, "A Four Element Phased Patch Antenna Array using Fluidic Phase Shifter" *URSI General Assembly and Scientific Symposium.*, August 2017.

[4] D. L. Diedhiou, R. Sauleau and A. V. Boriskin, "Microfluidically Tunable Microstrip Filters," *IEEE Trans. Microw. Theory Techn.*, vol. 63, no. 7, pp. 2245-2252, 2015.

[5] A. Pourghorban Saghati, J. S. Batra, J. Kameoka and K. Entesari, "A Miniaturized Microfluidically Reconfigurable Coplanar Waveguide Bandpass Filter With Maximum Power Handling of 10 Watts," *IEEE Trans. Microw. Theory Techn.*, vol. 63, no. 8, pp. 2515-2525, 2015.

[6] D. Rodrigo, L. Jofre and B. A. Cetiner, "Circular Beam-Steering Reconfigurable Antenna With Liquid Metal Parasitics," *IEEE Trans. Antennas Propag.*, vol. 60, no. 4, pp. 1796-1802, 2012.

[7] A. J. King et al "Microfluidically Switched Frequency-Reconfigurable Slot Antennas," in *IEEE Antennas Wireless Propag.Lett.*, vol. 12, pp. 828-831, 2013.

[8] M. Li and N. Behdad, "Fluidically Tunable Frequency Selective/Phase Shifting Surfaces for High-Power Microwave Applications," *IEEE Trans. Antennas Propag.*, vol. 60, no. 6, pp. 2748-2759, June 2012.